SINERGI Vol. 26, No. 1, February 2022: 23-30
http://publikasi.mercubuana.ac.id/index.php/sinergi
http://doi.org/10.22441/sinergi.2022.1.004

Numerical analysis of the vortex flow effect on the thermal-hydraulic performance of spray dryer

Fajar Anggara[1], Dedik Romahadi[1], Alief Avicenna Luthfie[1], Yosua Heru Irawan[2,3]
[1]Department of Mechanical Engineering, Faculty of Engineering, Universitas Mercu Buana, Indonesia
[2]Department of Mechanical Engineering, Faculty of Engineering, National Taiwan University of Science and Technology, Taiwan
[3]Department of Mechanical Engineering, Faculty of Engineering, Institut Teknologi Nasional Yogyakarta, Indonesia

Abstract
The use of a spray-dryer is very popular in the drying process in the food and beverage industry. However, due to the properties of the sensitive product that the quality will degrade in drying at high temperature, the innovative design of spray-dryer is developed which can increase the heat transfer rate at moderate temperature. This research was conducted to develop a spray-dryer design to improve thermal-hydraulic performance, with a high transfer rate and low-pressure drop at such a temperature. The design varies by several inlets categorized as design A with one inlet, design B with two inlets, and design C with three inlets. This simulation uses ANSYS FLUENT17, and the independence of the mesh was evaluated to improve the result of the simulation. The efficient mesh number is obtained from the independence of the mesh at around one million. The result shows that design C has the lowest pressure loss and the highest transfer rate due to high vortex and swirl flow generation, improving the mixture quality and direct contact between droplet and dry-air.

Keywords:
CFD;
Drying Process;
Sensitive Product;
Spray-Dryer;
Thermal-Hydraulic;
Vortex Flow;

Article History:
Received: March 10, 2021
Revised: August 27, 2021
Accepted: September 4, 2021
Published: February 1, 2022

Corresponding Author:
Fajar Anggara
Department of Mechanical Engineering, Universitas Mercu Buana, Indonesia
Email:
fajar.anggara@mercubuana.ac.id

INTRODUCTION

Spray dryers have been used widely in many industries such as food [1, 2, 3], beverage, and dairy [4]. As a result, many applications have been made using spray-dryers, such as encapsulation [1, 5, 6, 7], drying, and even cooling. However, the drying process using a spray-dryer has been challenging since a volatile product would degrade at drying high temperatures.

The advantages of spray dryers regarding the drying process are about eight times more economical than freeze-drying and four times more than vacuum drying [8] since less electric power consumption. Moreover, the other benefit is short, direct contact, which is important for preserving sensitive quality attributes such as nutrients, colour, and flavours [7][9].

Furthermore, the final product of the spray-dryer is very stable because of low moisture content and water activity [7]. Under this condition, it would reduce microbiological and degradation of oxidation [7][10].

The operating temperature in some applications industry operates between 150-220oC for inlet air dryer and outlet 50-80oC which could damage sensitive and volatile compounds, i.e., vitamin C, anthocyanins, lycopene, colours and flavours [11, 12, 13] even for cheese industry its operating temperature is between 180-190^{o}C [4].

Many innovative designs have been proposed using Computational Fluid Dynamics (CFD) to study and examine their performance on various models [14][15]. The previous study investigated different configurations of chamber design in spray dryers [2]. This study provides

that most studies recently used the κ-ε model as turbulence modelling, especially in 3D. Some chamber configuration developments were elaborated, such as a spray-dryer with a rotary atomizer [1, 16, 17]. The advantage of using a rotary atomizer compared to pressure nozzle spray is that more drying chamber volume is effectively used since its rotation helps the dispersion of droplets. In some cases, pressure or twin fluid nozzles produce a larger volume of distribution than rotary [7].

The other study examines four stages of spray-dryer using simulation, then the results are compared against validation of experiment [18]. The result shows good agreement between simulation and experiment. However, despite the agreement, the study did not explain the thermal-hydraulic performance of spray dryers.

Another case of investigation is about cyclone performance that uses CFD. It shows that increasing inlet number could decrease pressure loss and increase vortex and swirl generation [19]. The other research shows that increasing vortex and swirl generation could increase mixing compounds and heat transfer rate [17, 20, 21, 22].

Based upon the sensitive product problem and the effect of vortex-swirl flow that could enhance heat transfer, the novel design of spray-dryer was proposed in this study. The study was conducted to examine the design of a spray-dryer whether a varying number of inlets could increase heat transfer at moderate temperature by generating vortex and swirl flow enhancement. This study is also analyzing the thermal-hydraulic performance of spray-dryers.

METHOD

This part will discuss mathematical modelling, boundary condition, geometry variation and boundary condition, mesh generation and independence of mesh.

Mathematical Modeling

In this study, some equations are used. Since the modelling uses Discrete Phase Material (DPM), the modelling is divided into two parts. The first part is the continuous phase, and the other part is the discrete phase. After each part has been defined, the interaction between them is explained.

Governing equation of mass continuity, momentum and energy for a continuous phase is defined as follows:

$$\frac{\partial \rho u_i}{\partial x_i} = M_m \quad (1)$$

$$\frac{\partial (\rho u_i u_j)}{\partial x_i} = -\frac{\partial P}{\partial x_i} + \frac{\partial}{\partial x_i}\left[\mu\left(\frac{\partial u_i}{\partial x_j} + \frac{\partial u_j}{\partial x_i}\right) - \rho\overline{u_i' u_j'}\right] + M_F \quad (2)$$

$$\frac{\partial (\rho C_p u_i T)}{\partial x_i} = \frac{\partial}{\partial x_i}\left(k\frac{\partial T}{\partial x_i} - \rho\overline{u_i' T'}\right) + M_h + M_l \quad (3)$$

For Newtonian Fluid, the stress tensor in (2) and (3) are defined in the following:

$$\rho\overline{u_i' u_j'} = u_t\left(\frac{\partial u_i}{\partial x_j} + \frac{\partial u_j}{\partial x_i}\right) - \frac{2}{3}\delta_{ij}\frac{\partial u_l}{\partial x_l} \quad (4)$$

$$\rho\overline{u_i' T'} = \frac{u_t}{\sigma_T}\frac{\partial T}{\partial x_i} \quad (5)$$

Governing equations for discrete/dispersed phase are described in the following:

$$\frac{\partial u_{pi}}{\partial t} = C_D\frac{18\mu}{\rho_p d_p}\frac{Re}{24}(u_i - u_{pi}) + \frac{g_i(\rho_p - \rho)}{\rho_p} \quad (6)$$

Reynold number and drag coefficient are computed using these equations:

$$Re = \frac{\rho d_p |u_p - u|}{\mu} \quad (7)$$

$$C_D = a_1 + \frac{a_2}{Re} + \frac{a_3}{Re} \quad (8)$$

Modelling for the interaction between two phases is evaluated in the following, the rate of evaporation is governed by gradient diffusion:

$$N_i = k_c(C_{i,s} - C_{i,\infty}) \quad (9)$$

$C_{i,s}$ is a droplet in the surface while $C_{i,\sim}$ is a droplet in the bulk gas, both of them for vapour concentration is defined as $\frac{P_{sat}(T_p)}{RT_p}$ and $X_i\frac{P_{sat}(T_p)}{RT_p}$.

For finding k_c value, Nusselt number correlation can be used:

$$Nu_{AB} = \frac{k_c d_p}{D_{i,m}} = 20 + 0.6Re_d^{1/2}Sc^{1/3} \quad (10)$$

Heat transfer from dry air to droplet is updated with the energy balances as it follows:

$$m_p C_p\frac{dT_p}{dt} = hA_p(T_\infty - T_p) + \frac{dm_p}{dt}h_{fg} \quad (11)$$

Droplet boiling is formulated to predict boiling rate when the droplet has reached temperature boiling while the mass excess non-volatile fraction [23].

$$\frac{d(d_p)}{dt} = \frac{4k_\infty}{\rho_p C_{p,\infty} d_p}(1 + 0.23\sqrt{Re})ln\left[1 + \frac{C_{p,\infty}(T_\infty - T_p)}{h_{fg}}\right] \quad (12)$$

Turbulence modelling that is used in this study is κ-ε standard model because some researchers have used it and its results meet good agreement against experiment validation [2].

Geometry Variation and Boundary Condition

The geometry of the spray-dryer in this study is shown in Figure 1. The geometry dimension in centimetres and the spray dryer are divided into three parts: Upper part, middle part, and bottom part. The upper part has a function to generate vortex flow. The number inlet at this part is varied with 1,2,3 inlet or variation A, B and C respectively. In the middle part where the drying process takes place. The nozzle is placed at the centre so the droplet can contact to air dryer. The last is the bottom part, where dry air and droplet vapour come out from the outlet.

In this study, variation A has 0.003 kg/m, whereas B and C have 0.0015 kg/s and 0.001 kg/s of dry air. This difference arises to maintain the total mass flow rate at each variation (0.003 kg/s). The properties of the fluid are completely shown in Table 1.

The diameter inlet of each variation is different from having equal inlet velocity. For variation, A has 2.7 cm, and B and C have 1.35 cm and 0.9 cm, respectively.

In terms of the total mass flow rate being constant, it is to make sure that the sum of energy by mass from the air dryer for the drying process is equal.

Mesh Generation and Independency of Mesh

In terms of mesh generation, the three parts of the spray dryer are divided into three parts: the upper and middle parts are hex mesh, whereas the bottom part is tetrahedral mesh. The mesh generation is shown in Figure 2.

The concern of this study is to investigate vortex flow and the drying process that takes place in the upper and middle parts. Therefore, mesh generation in those places has to be hex mesh to reduce the error.

Despite the mesh generation, independence of the mesh must be conducted to increase the result of the simulation. This evaluation is conducted by comparing the temperature average of the middle part at different sizes of mesh.

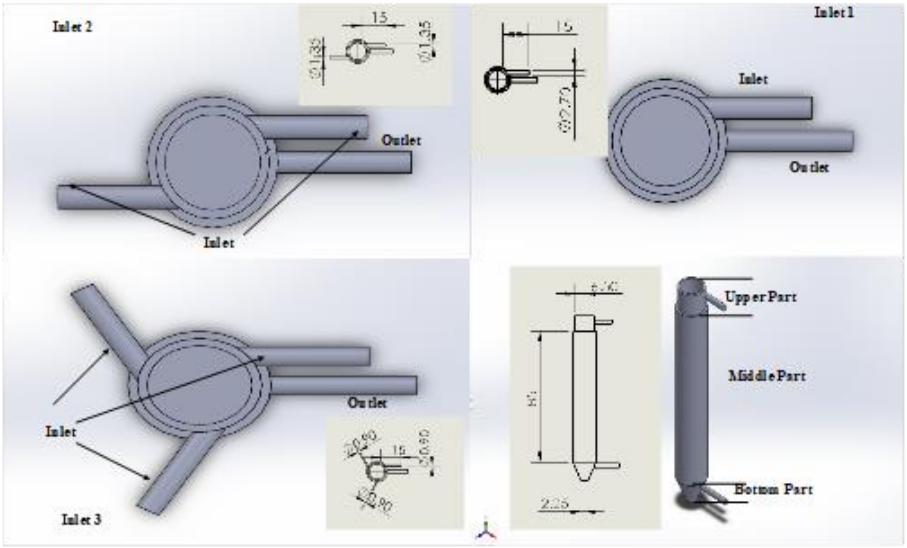

Figure 1. The geometry of the spray dryer

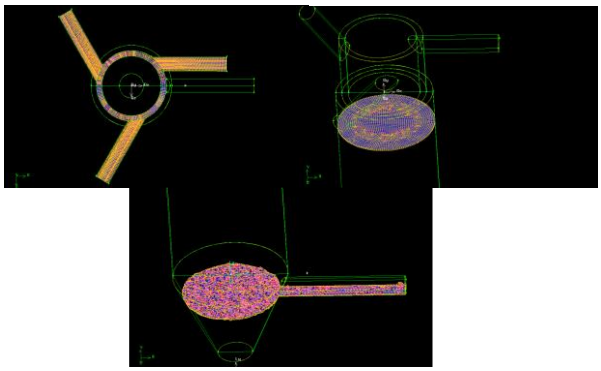

Figure 2. Mesh generation

Table 1. Properties of Fluid

Fluid	Variation		
	A	**B**	**C**
Dry Air	0.003 kg/s	0.0015 kg/s	0.001 kg/s
	60 C		
	1.225 kg/m3		
	0.0242 w/mK		
	1006.43 J/kgK		
Water Droplet	998.2 kg/m3		
	4182 J/kgK		
	10.85001 C Vap T		
	0.8 m/s		
	0.0003 kg/s		
	27 C		

Table 2. Evaluation of Independency of Mesh

Mesh Number	Temperature average of the middle part (°C)
234000	46.08
234000	46.08
444000	39.4234
1054000	45.937
4000000	46.261

Table 2 shows the evaluation of the independence of mesh. For example, when the number of mesh is 234000, the temperature average is 46.08 ^{0}C. Therefore, the number of mesh that is used in this study is 1054000 since there is a slightly different temperature average at 4 million mesh.

RESULTS AND DISCUSSION

This session will discuss the observation of velocity, temperature and pressure. Regarding on observation of velocity in the spray dryer, radial velocity contour is presented in Figure 3.

Figure 3 shows that variation C has the most uniform radial velocity distribution compared to other variations. By increasing the number of inlets, the flow could reach all around the upper part of the spray dryer then it could improve the distribution of radial velocity.

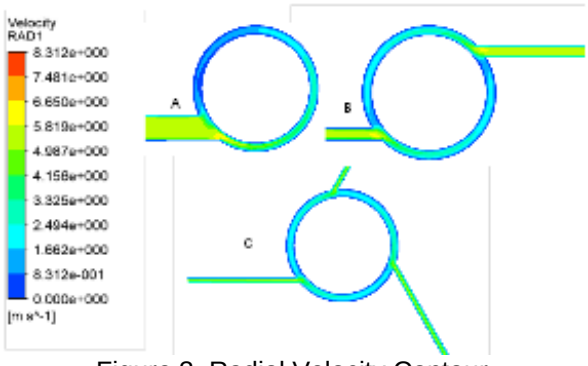

Figure 3. Radial Velocity Contour

Figure 4 shows the temperature contour in the axial direction. Gradient temperature shows in the middle part of the spray dryer, whereas evaporation occurs. This gradient temperature indicates a heat transfer from dry air to the droplet water throughout their interface while they contact each other. As a result, the droplet water phase changes into a vapour.

Gradient temperature will fade as the water droplet becomes vapour or temperature equilibrium between the droplet and dry air. For example, Figure 4 shows temperature equilibrium as the droplet is far away from the inlet. This is because dry air keeps transferring heat to droplets throughout the outlet.

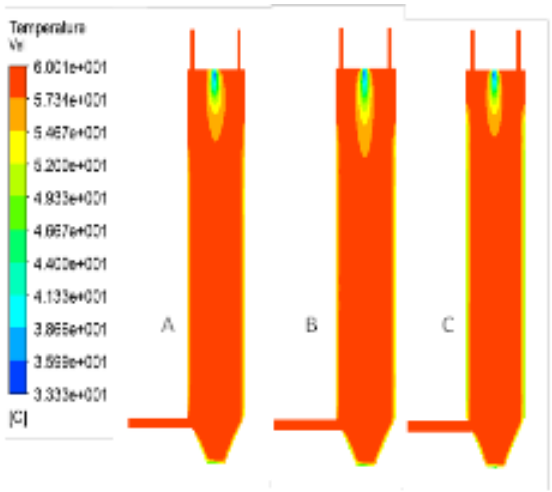

Figure 4. Axial Temperature Contour

The contour of radial temperature is presented in Figure 5. This contour is taken at the same height of each variation. It shows that the rate of drying process at variation C is the highest since the size of circular gradient temperature is the smallest. The same result for variation B occurs, as shown in Figure 5, that the evaporation rate is higher than variation A.

The correspondence between increasing the number of inlets and heat transfer rate is shown clearly in the Discrete Phase Material (DPM) report in FLUENT 17. The results are presented in Table 3.

Mass evaporation in Table 3. is calculated by evaluating mass continuity in the inlet and outlet. Therefore, it must be that the delta of mass transfer is positive due to the greater mass at the outlet due to the augment of evaporated water-droplet.

Table 3 shows that variation C has the most significant mass evaporation and the highest heat transfer rate. It indicates that increasing the number of inlets of the spray dryer would generate more uniform radial distribution and more vortex flow in the upper part of the spray dryer. Higher vortex flow generates swirl flow throughout the middle part of the spray dryer. As a consequence, heat transfer rate and droplet mass would increase.

The trajectories of droplet particles would describe why a higher transfer rate occurs at variations B and C, as shown in Figure 6.

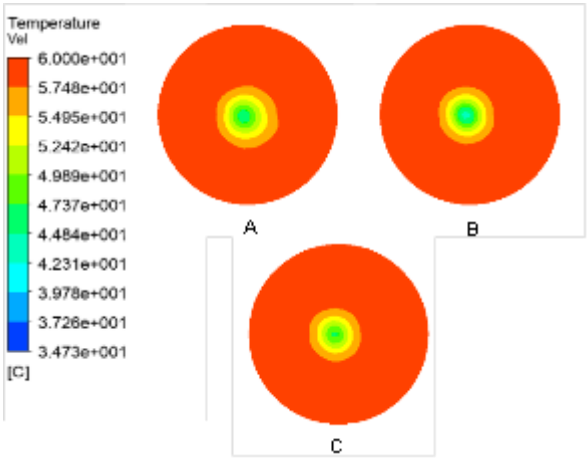

Figure 5. Radial Temperature Contour

Table 3. DPM Report

Variation	Mass Evaporation (kg/s)	Heat Transfer Rate (W)
A	0.0001219791	308.8667
B	0.0001261506	318.6511
C	0.0001327309	333.0964

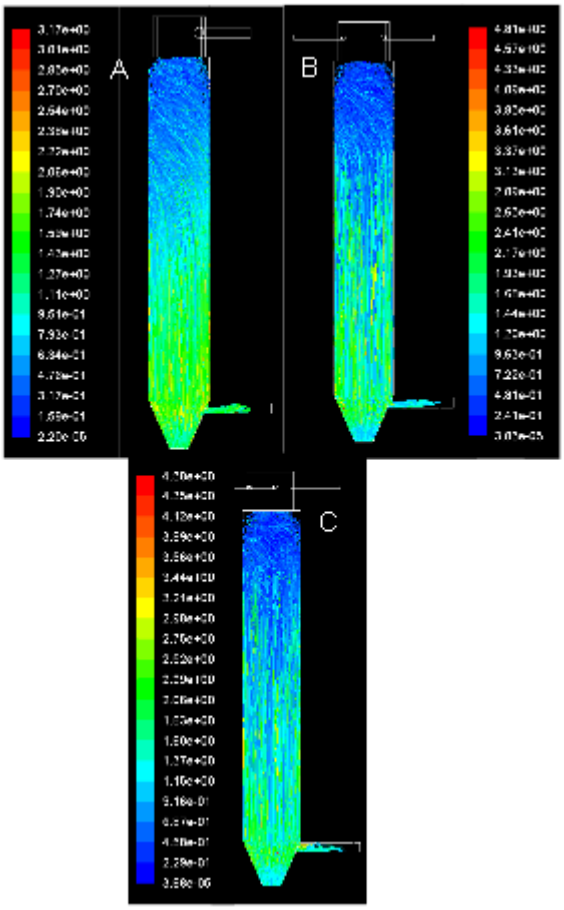

Figure 6. Particle Trajectory

Residence time is one of the reasons why such a heat transfer rate is achieved. Figure 6 shows that longer residence time occurs at variation B dan C due to higher vortex flow. Particle trajectory elaborates the higher vortex flow would induce and trap the droplet particle to stay in the middle part for a longer time. As a result, heat transfer from dry air would be improved as dry air and droplets would contact each other longer. However, the residence time of variation C is faster than variation B. It is because of the effect of the uniformity of velocity distribution. Hence, dry air would easily induce all particles throughout the middle part of the spray dryer.

Pressure loss will be examined in this study. The total pressure loss is tabulated in Table 4, which shows the highest-pressure loss occurred at variation A and the lowest pressure loss at variation C. This is because there is a reduction area due to circular paths making the flow collide with the wall as shown in the Figure 7. The collision in variation A has a more significant impact on the pressure gradient than other variations due to a bigger diameter inlet.

Table 4. Total Pressure Drop

Variation	Pressure Drop (Pascal)
A	42.47
B	12.14
C	6.44

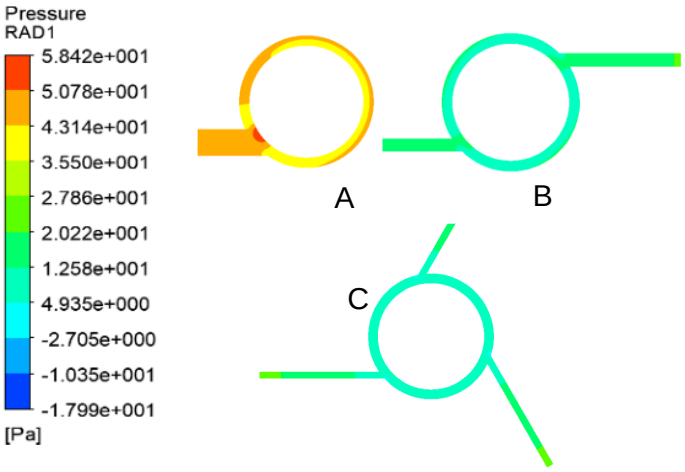

Figure 7. Radial Pressure Contour

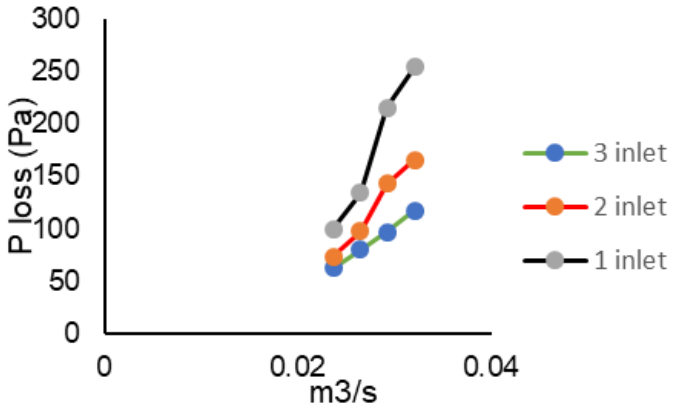

Figure 8. Total P loss [19]

This study's total pressure drop is aligned with previous study [19] in Figure 8, where three inlets have the smallest pressure drop.

CONCLUSION

Numerical simulation on thermal-hydraulic performance has been presented in this study. The novel design of spray-dryer has been proposed to answer the problem of volatile and sensitive products in the drying process. In which due to sensitive quality attributes will damage at a higher temperature. It is shown in this study, based on thermal-hydraulic performance, that increasing the number of inlets would improve heat transfer from dry air. It is shown the highest heat transfer rate on variation C (333.1 Watt). This is the consequence of higher vortex and swirl generation flow that trap droplet particles to absorb heat from dry air for a longer time.

The best design in this study has thermal-hydraulic performance, whereas it has the best-improving heat transfer (333.1 Watt) and the lowest pressure drop (6.44 Pa) is variation C. However, another problem would arise: the resident time is deficient in the study. Therefore, incoming next research will focus not only on thermal-hydraulic performance but also on improving the resident time. The next research investigates the effect of mass flow rate and temperature of dry air in the drying process using three inlets.

ACKNOWLEDGMENT

This research was supported by the Research Center of Universitas Mercu Buana,

which gives a grant in internal research. We thank our National Taiwan University of Science and Technology colleagues, who provided insight and expertise that greatly assisted the research.

REFERENCES

[1] A. G. Gaonkar, N. Vasisht, A. R. Khare, and R. Sobel, *Microencapsulation in the Food Industry A Practical Implementation Guide*, vol. 53. 2014.

[2] R. Kuriakose and C. Anandharamakrishnan, "Computational fluid dynamics (CFD) applications in spray drying of food products," *Trends in Food Science & Technology*, vol. 21, no. 8, pp. 383–398, 2010, doi: 10.1016/j.tifs.2010.04.009.

[3] T. A. G. Langrish and D. F. Fletcher, "Spray drying of food ingredients and applications of CFD in spray drying," *Chemical Engineering Process*, vol. 40, no. 4, pp. 345–354, 2001, doi: 10.1016/S0255-2701(01)00113-1.

[4] J. Písecký, "Spray drying in the cheese industry," *International Dairy Journal*, vol. 15, no. 6–9, pp. 531–536, 2005, doi: 10.1016/j.idairyj.2004.11.010.

[5] P. Schuck *et al.*, "Recent advances in spray drying relevant to the dairy industry: A comprehensive critical review," *Dry Technology*, vol. 34, no. 15, pp. 1773–1790, 2016, doi: 10.1080/07373937.2016.1233114.

[6] J. J. O'Sullivan, E. A. Norwood, J. A. O'Mahony, and A. L. Kelly, "Atomisation technologies used in spray drying in the dairy industry: A review," *Journal of Food Engineering*, vol. 243, pp. 57–69, 2019, doi: 10.1016/j.jfoodeng.2018.08.027.

[7] M. R. I. Shishir and W. Chen, "Trends of spray drying: A critical review on drying of fruit and vegetable juices," *Trends in Food Science & Technology*, vol. 65, pp. 49–67, 2017, doi: 10.1016/j.tifs.2017.05.006.

[8] C. Santivarangkna, U. Kulozik, and P. Foerst, "Alternative drying processes for the industrial preservation of lactic acid starter cultures," *Biotechnology Progress*, vol. 23, no. 2, pp. 302–315, 2007, doi: 10.1021/bp060268f.

[9] G.R. Rodríguez-Hernández, R. González-García, A. Grajales-Lagunes, M.A. Ruiz-Cabrera* & M. Abud-Archila, "An Spray-Drying of Cactus Pear Juice (Opuntia streptacantha): Effect on the Physicochemical Properties of Powder and Reconstituted Product," *Drying Technology*, vol. 23, no. 4, pp. 955–973, 2005, doi: 10.1080/DRT-200054251

[10] L. G. Marques, M. C. Ferreira, and J. T. Freire, "Freeze-drying of acerola (Malpighia glabra L.)," *Chemical Engineering and Processing: Process Intensification*, vol. 46, no. 5, pp. 451–457, 2007, doi: 10.1016/j.cep.2006.04.011.

[11] V. Patil, A. K. Chauhan, and R. P. Singh, "Optimization of the spray-drying process for developing guava powder using response surface methodology," *Powder Technology*, vol. 253, pp. 230–236, 2014, doi: 10.1016/j.powtec.2013.11.033.

[12] W. Chen, J. Zhao, T. Bao, J. Xie, W. Liang, and V. Gowd, "Comparative study on phenolics and antioxidant property of some new and common bayberry cultivars in China," *Journal of Functional Foods*, vol. 27, pp. 472–482, 2016, doi: 10.1016/j.jff.2016.10.002.

[13] T. Bao *et al.*, "Systematic study on phytochemicals and antioxidant activity of some new and common mulberry cultivars in China," *Journal of Functional Foods*, vol. 25, pp. 537–547, 2016, doi: 10.1016/j.jff.2016.07.001.

[14] A. A. Luthfie, D. Romahadi, H. Ghufron, and S. D. Murtyas, "Numerical Simulation on Rear Spoiler Angle of Mini Mpv Car for Conducting Stability and Safety," *SINERGI*, vol. 24, no. 1, p. 23, 2019, doi: 10.22441/sinergi.2020.1.004.

[15] B. Metheny, R. Permatasari, and M. S. Annas, "Design Modeling of Savonius-Darrieus Turbine for Sea Current Electric Power Plant," *SINERGI*, vol. 25, no. 1, p. 27, 2020, doi: 10.22441/sinergi.2021.1.004.

[16] T. Defraeye, "Advanced computational modelling for drying processes - A review," *Applied Energy*, vol. 131, pp. 323–344, 2014, doi: 10.1016/j.apenergy.2014.06.027.

[17] L. X. Huang, M. L. Passos, K. Kumar, and A. S. Mujumdar, "A three-dimensional simulation of a spray dryer fitted with a rotary atomizer," *Dry Technology*, vol. 23, no. 9–11, pp. 1859–1873, 2005, doi: 10.1080/07373930500210176.

[18] L. N. Petersen, N. K. Poulsen, H. H. Niemann, C. Utzen, and J. B. Jørgensen, "An experimentally validated simulation model for a four-stage spray dryer," *Journal of Process Control*, vol. 57, pp. 50–65, 2017, doi: 10.1016/j.jprocont.2017.05.001.

[19] H. Safikhani, J. Zamani, and M. Musa, "Numerical study of flow field in new design cyclone separators with one , two and three tangential inlets," *Advanced Powder Technology*, no. December, 2017, doi: 10.1016/j.apt.2017.12.002.

[20] B. Hernandez, B. Fraser, L. Martin De Juan, and M. Martin, "Computational Fluid Dynamics (CFD) Modeling of Swirling Flows in Industrial Counter-Current Spray-Drying Towers under Fouling Conditions †," *Industrial & Engineering Chemistry Research,* vol. 57, no. 35, pp. 11988–12002, 2018, doi: 10.1021/acs.iecr.8b02202.

[21] V. Francia, L. Martin, A. E. Bayly, and M. J. H. Simmons, "An experimental investigation of the swirling flow in a tall-form counter current spray dryer," *Experimental Thermal and Fluid Science*, vol. 65, pp. 52–64, 2015, doi: 10.1016/j.expthermflusci.2015.03.004.

[22] M. Sheikholeslami, M. Gorji-Bandpy, and D. D. Ganji, "Review of heat transfer enhancement methods: Focus on passive methods using swirl flow devices," *Renewable and Sustainable Energy Reviews*, vol. 49, pp. 444–469, 2015, doi: 10.1016/j.rser.2015.04.113.

[23] ANSYS Inc. (US), "Ansys Users' Guide," *Aging (Albany. NY).*, vol. 7, no. 11, pp. 956–963, 2015, doi: 10.1017/ CBO9781107415324.004.